

Overcoming Current Quantization Effects for Precise Current Control by Extended Dithering Techniques

*Hongzhong Zhu(The University of Tokyo) Fujimoto Hiroshi (The University of Tokyo)

Abstract– Precise current control and motor sensorless control need accurate current signals. However, current measurement error including the metering error and the quantization error is unavoidable for digital control. In this paper, extended dithering techniques are presented to suppress the quantization effects caused by A/D converters. It is shown that by the use of dither having a suitably chosen probability density function, the total measurement error can be rendered spectrally white while the variance of the total error is minimized. The effectiveness of the proposed methods is verified by simulations and experiments.

Key Words: dithering techniques, quantization, analog-to-digital converter, current control

1 Introduction

Precise current measurement is essential for current control and motor sensorless control to produce high static and dynamic performance of ac motor drive systems. As the current measurement error is introduced into the control system by current sensors and A/D converters (ADC), the real current signals of a motor are not guaranteed to follow the reference values exactly. This would cause torque ripple and deteriorate the control performance especially at low load [2, 3]. Therefore, understanding and suppressing the current measurement error have attracted a great deal of attention, see, e.g., [1, 4, 5].

Current measurement error can be classified as the metering error and the quantization error. The metering error, which is caused by thermal drift, dc offset and scaling inaccuracy, is introduced into control loop by current sensors and other analog devices. The quantization error arises because the analog current signal may assume any value within the input range of the A/D converters while the output data is a sequence of finite precision samples. Quantization error behaves as highly colored noise and cannot be ignored in many cases. It is reported in [4] that quantization error would affect the accuracy of the rotor position estimation when high frequency signal injection method is used for sensorless control.

It is known that white noise is easier to deal with than other colored noise because it contains equal power at any center frequency. Many methods, such as Kalman filter and LQG design methods, are proposed based on the assumption that the noises introduced to the system are white. Motivated by this perspective, in this paper, dithering techniques are exploited to suppress the quantization effects. Subtractively dithered system and nonsubtractively dithered system are respectively designed to render the quantization error be spectrally white and to minimize the variance of the total current error by taking into account the statistical properties of the metering error. Their effectiveness is validated via simulations and experiments.

The remainder of this paper is organized as follows. Section 2 presents some important theorems referring to quantization and dither. The current measurement is analyzed and the extended dithering techniques are proposed in Section 3. Sections 4 and 5 demonstrate the effectiveness of the proposed extended dithering techniques on current quantization via simulations and experiments. Finally, conclusion is given in Section 6.

2 Preliminaries

2.1 Quantization

An ideal ADC is a nonlinear device having a staircase-type I/O relation, as shown in Fig. 1. The amplitude of an input signal is arbitrary and the possible amplitude of output signal is countably finite number of values. Assuming that the input is always within the measurement range of ADCs, an ideal ADC can be expressed in terms of the input x and the quantization step Δ as

$$Q(x) = \Delta \lfloor \frac{x}{\Delta} + \frac{1}{2} \rfloor, \quad (1)$$

where $Q(\cdot)$ is the quantizing operation. The quantization error is defined by

$$\begin{aligned} q &\triangleq y - x \\ &= Q(x) - x, \end{aligned} \quad (2)$$

where x is the input, y is the output. q is dependent of x unless x satisfies the so-called band-limited condition, which is also referred to as the "Quantization Theorem" [9]. The band-limitedness assumption on the input is not satisfied universally. Although q is usually highly colored, its classical model treats it as a random process with a probability density function (pdf)

$$p_q(\epsilon) = \begin{cases} \frac{1}{\Delta}, & -\frac{\Delta}{2} < \epsilon \leq \frac{\Delta}{2} \\ 0, & \text{otherwise.} \end{cases} \quad (3)$$

Based on this kind of treatment, the mean and the variance of the quantization error are [7]

$$E[q] = 0, \quad (4)$$

$$E[q^2] = \frac{\Delta^2}{12}. \quad (5)$$

This treatment is valid for complex input signals whose amplitudes are large relative to the quantization step Δ . However, it fails catastrophically for small or simple signals.

2.2 Dither

Dither, which is an intentionally applied form noise, can decorrelate signal-dependent noise such as quantization noise, has been wildly applied in the past fifty years to suppress the quantization effects on audio or video signal processing [6, 7, 10]. There exist two archetypes of dithering systems: subtractively

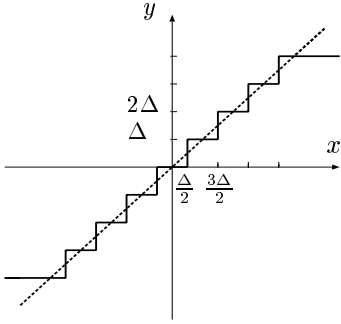


Fig. 1: Quantization characteristic. Δ is the quantization step.

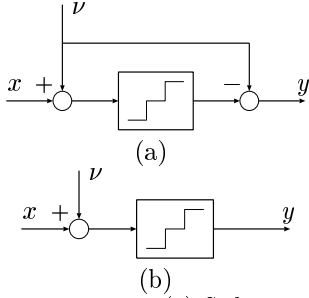


Fig. 2: Dithering systems. (a) Subtractively dithered system; (b) Nonsubtractively dithered system. x is the system input, and y is the system output.

dithered system and nonsubtractively dithered system. Schematics of these systems are shown in Fig. 2. In the subtractively dithered system, the total error is given by

$$\begin{aligned} e &= y - x \\ &= Q(x + \nu) - (x + \nu) \\ &= q(x + \nu), \end{aligned} \quad (6)$$

where ν denotes the dither. Note that the statistical properties of the dither can be chosen to control the properties of the error. In particular, it can be shown that [6]:

Schuchman's Condition: In a subtractively dithered quantizing system, the total error e is uniformly distributed and statistically independent of the input for arbitrary input distributions if and only if the characteristic function of the dither, P_ν , satisfies the condition that

$$P_\nu(u)|_{u=k/\Delta} = 0, \quad \text{for } k = \pm 1, \pm 2, \pm 3, \dots \quad (7)$$

The characteristic function of a random variable is the Fourier transform of its pdf p_ν , which is defined by

$$P_\nu(u) \triangleq \int_{-\infty}^{\infty} p_\nu(\epsilon) e^{-j2\pi u \epsilon} d\epsilon. \quad (8)$$

Note that a dither with the uniform probability distribution

$$p_\nu(\epsilon) = \begin{cases} \frac{1}{\Delta}, & -\frac{\Delta}{2} < \epsilon \leq \frac{\Delta}{2} \\ 0, & \text{otherwise,} \end{cases} \quad (9)$$

has the corresponding characteristic function

$$P_\nu = \frac{\sin(\pi \Delta u)}{\pi \Delta u}, \quad (10)$$

which satisfies the desired condition (7). Applying this sort of dither can made the total error e be independent of input x . In addition, the mean and the variance of the total error e are as same as (4) and (5).

Subtractively dithered systems are clearly ideal in the sense that they render the total error e be independent of the input. The requirement of synchronous dither subtraction at the system output, however, cannot always be implementable in practical situations. It is for such reasons, nonsubtractive dither technique introduced in the following is also of interest.

In the case of nonsubtractively dithered system, the total error can be given by

$$\begin{aligned} e &= y - x \\ &= Q(x + \nu) - x \\ &= q(x + \nu) + \nu. \end{aligned} \quad (11)$$

Obviously the total error is not simply the quantization error alone, but also involves the dither. Unlike subtractive dithering method, it is shown that nonsubtractive dithering method cannot make the total error statistical independent of the system input [8]. However, the following result can be obtained [7]:

Theorem: In a nonsubtractively dithered quantizing system, $E[e^l|x]$ is functionally independent of the input x for $l = 1, 2, \dots, M$ if and only if

$$\frac{d^i P_\nu}{d u^i}(u) \Big|_{u=k/\Delta} = 0 \quad \text{for } k = \pm 1, \pm 2, \pm 3, \dots, \quad (12)$$

where $i = 0, 1, 2, \dots, M - 1$.

Based on this **Theorem**, the mean and the variance of the total error are expressed as follows:

$$E[e] = E[\nu], \quad (13)$$

$$E[e^2] = E[\nu^2] + \frac{\Delta^2}{12}. \quad (14)$$

It is analyzed in [8] that triangular-pdf dither of 2-LSB peak-to-peak amplitude

$$p_w(\epsilon) = \begin{cases} \frac{1}{\Delta^2}(\epsilon + \Delta), & -\Delta < \epsilon \leq 0 \\ \frac{1}{\Delta^2}(-\epsilon + \Delta), & 0 < \epsilon \leq \Delta \\ 0, & \text{otherwise,} \end{cases} \quad (15)$$

is unique choice to render the mean and the variance of the total error e be independent of the input, while minimizing the variance. In this case, they are given by

$$E[e] = 0, \quad (16)$$

$$E[e^2] = \frac{\Delta^2}{4}. \quad (17)$$

3 Dithering techniques for current quantization

3.1 Current measurement

In this section, current measurement for digital current control is analyzed. Extended dithering techniques are proposed by taking account of the statistical properties of the metering error.

Fig. 3 shows the typical path of the current measurement [11]. Current signals, transduced to the

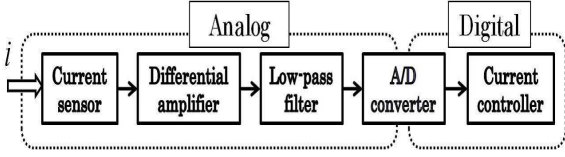


Fig. 3: Path of current measurement.

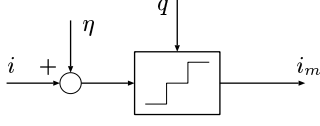


Fig. 4: Model of the current measurement: η is the metering error, and q is the quantization error.

voltage signals by current sensors, are transformed into digital values via A/D converters after amplitude amplification and noise filtering. During this procedure, the metering error and the quantization error are introduced to the control system, as shown in Fig. 4. The metering error, which is mainly caused by thermal drift by analog devices, is denoted by η . Without loss of generality, the real current value is assumed to be within the measuring range of current sensors, which means that the metering accuracy is guaranteed.

The quantization step Δ in this case can be expressed by

$$\Delta = \frac{I_0}{2^{N_b-1}}, \quad (18)$$

where I_0 is parameter of the measurement range $\pm I_0$, and N_b is the resolution of an A/D converter. In the following, the dithering techniques are considered to be applied on suppressing the current quantization effects.

3.2 Subtractively dithered system

As introduced in the last section, subtractive dithering method is ideal for suppressing quantization effects because that it can make the quantization noise be independent of input as well as the variance of the total error is not enlarged. Its application on suppressing current quantization is shown in Fig. 5. The current error is expressed as

$$\begin{aligned} e_i &= i_m - i \\ &= Q(i_\eta + \nu) - (i_\eta + \nu) + \eta \\ &= q(i_\eta + \nu) + \eta. \end{aligned} \quad (19)$$

According to **Schuchman's Condition**, $q(i_\eta + \nu)$ is independent of i_η if ν is uniform noise shown as (9). Therefore, if the metering error η can be assumed to be white noise, the total current measurement error e_i would be regarded as white noise. The mean and the variance of e_i are expressed as

$$E[e_i] = 0, \quad (20)$$

$$E[e_i^2] = E[\eta^2] + \frac{\Delta^2}{12}. \quad (21)$$

3.3 Nonsubtractively dithered system

The application of nonsubtractively dithered method is considered in this subsection. The block diagram is shown in Fig. 6. Denote the sum of the dither ν and the metering error η by

$$w \triangleq \eta + \nu, \quad (22)$$

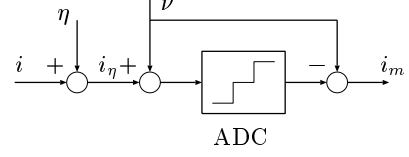


Fig. 5: Model of subtractive dithering method for current measurement system.

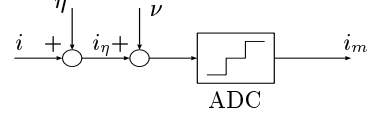


Fig. 6: Model of nonsubtractive dithering method for current measurement system.

for the sake of convenience. In order to make the mean and the variance of the total error e_i be independent of the input as well as to minimize the variance of e_i , the statistical properties of η is taken into account. According to the **Theorem** presented in the last section, the optimal selection of ν is the one which can control w to be the triangular-pdf noise (15). According to convolution theorem and inverse Fourier Transform, a theoretical optimal selection of ν can be computing by

$$p_\nu = \mathcal{F}^{-1} \frac{\text{sinc}^2(\pi\Delta u)}{P_\eta(u)} du, \quad (23)$$

where $\text{sinc}^2(\pi\Delta u)$ and $P_\eta(u)$ are the characteristic function of triangular-pdf (15) and η , respectively. \mathcal{F}^{-1} denotes the inverse Fourier Transform. A variable with the probability distribution solved from (23) is usually not so easy to implement. According to the practical situation, two common cases that η is uniform noise and η is Gaussian noise are discussed, respectively.

3.3.1 The metering error is uniform noise

In this case, the following **proposition** can be obtained:

Proposition 1: Suppose that η is uniform noise with the probability distribution

$$p_\eta(\epsilon) = \begin{cases} \frac{N}{\Delta}, & -\frac{\Delta}{2N} < \epsilon \leq \frac{\Delta}{2N} \\ 0, & \text{otherwise,} \end{cases} \quad (24)$$

where $N \in \mathcal{N}$ is a natural number, then w is the triangular-pdf noise expressed by (15) if the probability distribution of ν satisfies

$$p_\nu(\epsilon) = \begin{cases} \frac{1}{N\Delta}, & \begin{cases} -\frac{2N-1}{2N}\Delta < \epsilon \leq -\frac{2N-3}{2N}\Delta \\ \frac{2N-3}{2N}\Delta < \epsilon \leq \frac{2N-1}{2N}\Delta \end{cases} \\ \frac{2}{N\Delta}, & \begin{cases} -\frac{2N-3}{2N}\Delta < \epsilon \leq -\frac{2N-5}{2N}\Delta \\ \frac{2N-5}{2N}\Delta < \epsilon \leq \frac{2N-3}{2N}\Delta \end{cases} \\ \vdots & \vdots \\ \frac{i}{N\Delta}, & \begin{cases} -\frac{2(N-i)+1}{2N}\Delta < \epsilon \leq -\frac{2(N-i)-1}{2N}\Delta \\ \frac{2(N-i)-1}{2N}\Delta < \epsilon \leq \frac{2(N-i)+1}{2N}\Delta \end{cases} \\ \vdots & \vdots \\ \frac{N-1}{N\Delta}, & \begin{cases} -\frac{3}{2N}\Delta < \epsilon \leq -\frac{1}{2N}\Delta \\ \frac{1}{2N}\Delta < \epsilon \leq \frac{3}{2N}\Delta \end{cases} \\ \frac{1}{\Delta}, & -\frac{1}{2N}\Delta < \epsilon \leq \frac{1}{2N}\Delta \\ 0, & \text{otherwise,} \end{cases} \quad (25)$$

where $i = 1, 2, \dots, N-1$. Fig. 7 shows the convolution of p_η and p_ν to form p_w in the case of $N = 2$.

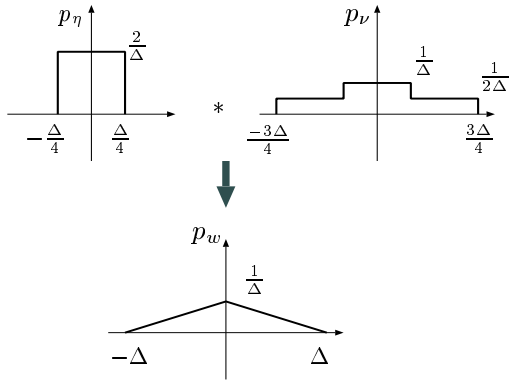


Fig. 7: Example of **Proposition 1** in the case of $N = 2$.

Proof: According to the Convolution theorem, this proposition can be easily proved.

Note that the metering error $|\eta| \leq \frac{\Delta}{2}$ is only considered in (24). If the metering error is larger, ν can also be designed to render the total error e_i be functionally independent of true input if the **Theorem** in Section 2 is satisfied. However, the SNR may be too low to acceptable.

3.3.2 The metering error is Gaussian noise

In this case, designing ν based on (23) is very hard not only because of the calculation, but also the realization for practical situation. Therefore, controlling ν to make w fit the probability distribution (15) is considered. The simplest way is to set w as Gaussian noise with the same variance as the triangular-pdf noise (15). According to the convolution theorem and the properties of Normal distribution, the following results can be obtained:

Proposition 2: Suppose that the metering error η has the Normal distribution:

$$p_\eta(\epsilon) = \frac{1}{\sqrt{2\pi\sigma^2}} e^{-\frac{1}{2}\frac{\epsilon^2}{\sigma^2}}, \quad 0 < \sigma^2 < \frac{\Delta^2}{6}, \quad (26)$$

where σ is the standard deviation, w has the same variance as the triangular-pdf noise (15). if the probability distribution of ν satisfies

$$p_\nu(\epsilon) = \frac{1}{\sqrt{2\pi(\frac{\Delta^2}{6} - \sigma^2)}} e^{-\frac{1}{2}\frac{\epsilon^2}{\frac{\Delta^2}{6} - \sigma^2}}. \quad (27)$$

4 Simulations

In this section, the simulations are performed to verify the effectiveness of the extended dithering techniques presented in the last section. The models shown in Fig. 5 and Fig. 6 are exploited. An ADC with a resolution of 10 bits and the measurement range of $\pm 50A$ is considered. The corresponding quantization step is $\Delta = 0.0977A$ according to (18). The input current signal is set as $i^* = \sin 10\pi t$.

Firstly, the metering error η which is set as uniform noise with the distribution shown in Fig. 7 is considered. Without dither, with the subtractive dither designed via (9), and with the nonsubtractive dither designed via (25) are performed, respectively. In the case that without dither, there are sharp peaks fall at multiples of the input sine wave frequency, as shown in Fig. 8(a). The results of applying subtractive dither and nonsubtractive dither are shown in Figs. 8(b,c).

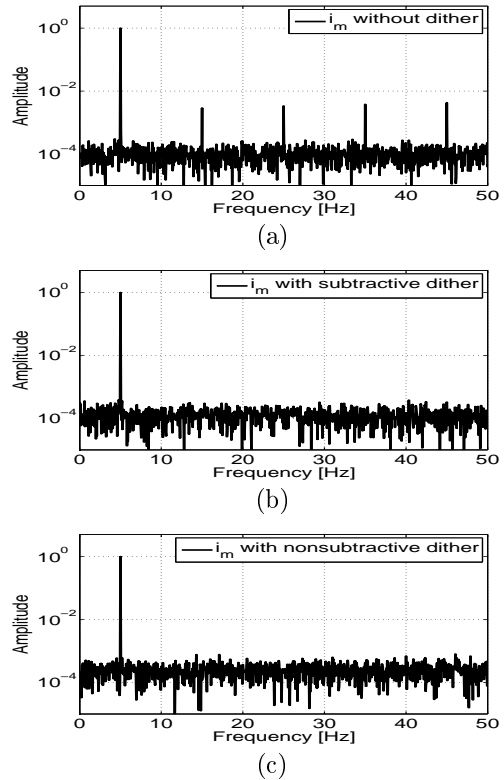


Fig. 8: Simulation results in the case that the metering error is uniform noise with $|\eta| \leq \frac{\Delta}{4}$. (a) shows the feature of quantized current signal without applying dither. (b) shows the result when subtractive dither (9) is applied. (c) shows the result when nonsubtractive dither (25) is applied.

Table 1: Parameters of stage

Inductance L	6.4×10^{-3}	H
Resistance R	13.1	Ω
Mass M	14.3	kg
Viscosity B	24	$N/(m/s)$
Thrust coefficient K_t	26.5	N/A
Bach-EMF constant K_e	9.5	$V/(m/s)$

It is observed that the sharp peaks are reduced, which implies that both the subtractive dither and the non-subtractive dither can render the quantization noise to be spectrally white.

Then, the metering error η is set as the Normal distribution $N(0, \frac{\Delta^2}{48})$, which has the same variance as uniform noise of $|\eta| \leq \frac{\Delta}{4}$. Without dither, with the subtractive dither designed via (9), and with the nonsubtractive dither designed via (27) are examined. The simulation results are shown in Fig. 9. It is also observed that the sharp peaks are suppressed, and the effectiveness of the subtractive dithering method and the nonsubtractive dithering method is verified.

5 Experiments

In this section, the effectiveness of extended dither techniques are verified via experiments. The experimental setup is shown in Fig. 10, whose parameters are shown in Table. 1. The stage is driven by linear motors located at the two sides of the carrier. The position information is measured by an encoder

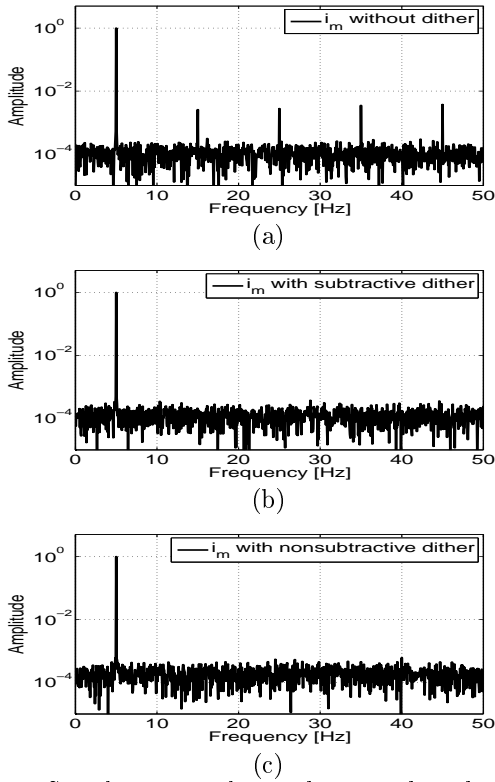


Fig. 9: Simulation results in the case that the metering error is Gaussian noise with variation $\sigma^2 = \frac{\Delta^2}{48}$. (a) shows the feature of quantized current signal without applying dither. (b) shows the result when subtractive dither (25) is applied. (c) shows the result when nonsubtractive dither (27) is applied.

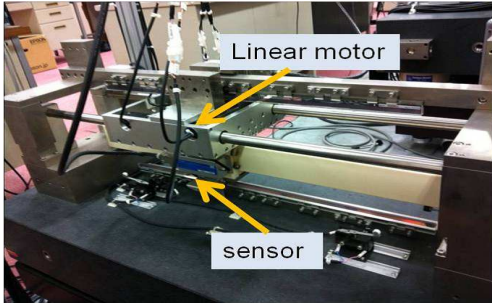


Fig. 10: The experimental setup.

with the resolution of 1 nm. U-phase and W-phase currents are measured by FA-050PV and then converted into digital signal by an A/D converter whose resolution is 14 bits. The resolution is dropped to 10 bits by software for the convenience of comparison. Dither is generated by DSP and then converted to analog signal via D/A converter whose resolution is 16 bits. The implementation of the subtractive dither method is shown in Fig. 11. A time delay is also introduced to synchronize the addition and the subtraction. The position controller, speed controller and current controller are designed in advance. The block diagram of control system is shown in Fig. 12.

Firstly, the metering error is measured by the ADC with the resolution of 14 bits. the histogram plot of the noise is shown in Fig. 13. It is observed that the metering error can be regarded as Gaussian noise. The corresponding variance is 1.1218×10^{-4} . Based on this value, the nonsubtractive dither and

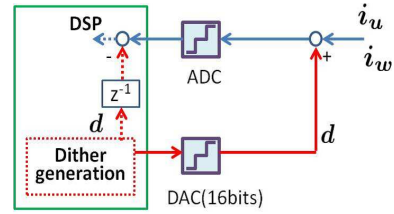


Fig. 11: The implement of subtractive dither method.

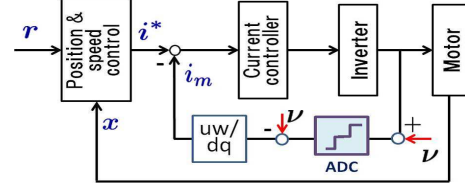


Fig. 12: Block diagram of control system.

subtractive dither are designed according to (27) and (9).

The trajectory of the stage is set linearly, as shown in Fig. 14. The corresponding velocity reference is constant. The experimental results are shown in Figs. 15 ~ 16. The solid line shows the results of 10 bits ADC without dither. The dotted line shows the result of 10 bits ADC with subtractive dither. The dashed line shows the results of 10 bits ADC with nonsubtractive dither. It is observed from Fig. 15 that the components at high frequencies are reduced if dithering techniques are applied, which also means that the ripple caused by current quantization can be suppressed. the RMS of the tracking errors are shown in Table 2. It is shown that both subtractively dithered method and nonsubtractively dithered method can reduce the current quantization effects. The subtractive dither method can obtain a relatively small tracking error.

Table 2: The RMS of tracking error with & without dither

	10-bit w/o dither	10-bit w/ sub. d	10-bit w/ nsub. d
tracking error (μm)	4.4299	3.4265	3.9513

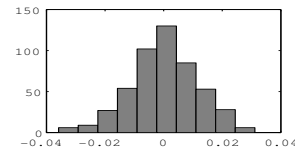


Fig. 13: Histogram plot of the metering error by using an ADC with the resolution of 14 bits.

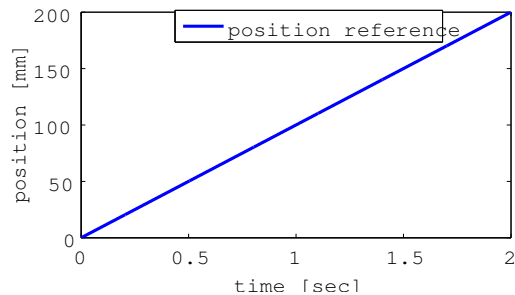


Fig. 14: The position reference.

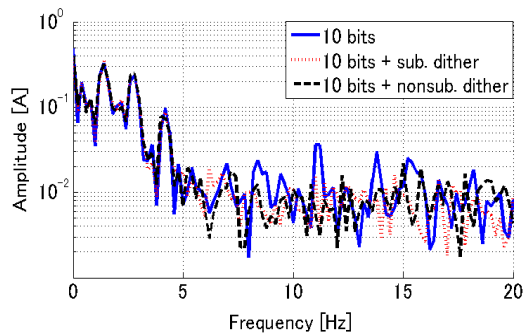


Fig. 15: FFT of U-phase current signals. The solid line shows the results of 10 bits ADC without dither. The dotted line shows the result of 10 bits ADC with subtractive dither. The dashed line shows the results of 10 bits ADC with nonsubtractive dither.

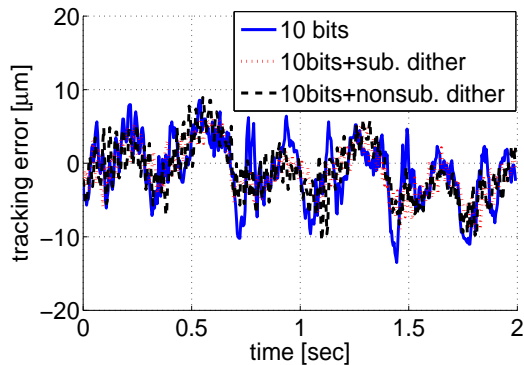


Fig. 16: The comparison of the position tracking error. The solid line shows the results of 10 bits ADC without dither. The dotted line shows the result of 10 bits ADC with subtractive dither. The dashed line shows the results of 10 bits ADC with nonsubtractive dither.

6 Conclusion

In this paper, some significant theorems on quantization and dithering techniques are reviewed, and their applications on current quantization are presented. In order to make the current measurement error be independent of real current signal and minimize its variance, extended dithering techniques are proposed by taking into account the statistical properties of the metering error. According to the simulation results, the proposed methods can render the total measurement error be spectrally white. The dithering techniques are also applied to a high-precise stage, and the experimental results demonstrate their effectiveness.

References

- [1] D.W. Chung, and S.K. Sul, Analysis and Compensation of Current Measurement Error in Vector-Controlled AC Motor Drives *IEEE Trans. Indust. Appl.* , Vol. 34, No. 2, pp. 340–345, Mar./Apr. 1998.
- [2] J. Holtz, and J. Quan, Sensorless Vector Control of Induction Motors at Very Low Speed Using a Non-linear Inverter Model and Parameter Identification, *IEEE Trans. Indust. appl.* , Vol. 38, No. 4, pp. 1087–1095, Jul./Aug. 2002.
- [3] K. Nakamura, H. Fujimoto, and M. Fujisuna, Torque Ripple Suppression Control for PM Motor Considering the Bandwidth of Torque Meter (in Japanese), *IEEJ Trans. IA* , Vol. 130, No. 11 pp. 1241–1247, 2010.
- [4] J.H. Jang, S.K. Sul, and Y.C. Son, Current Measurement Issues in Sensorless Control Algorithm using High Frequency Signal Injection Method, *Proc. IEEE Ind. App. Soc. Annual Meeting* , Vol.2 pp. 1134–1141, Oct. Salt Lake City, 2003.
- [5] D. Antic, J. B. Klaassens, and W. Deleroi, Side effects in low-speed AC drives, *Conf. Rec. IEEE-PESC Meeting.* , pp. 998–1002, 1994.
- [6] L. Schuchman, Dither Signals and Their Effect on Quantization Noise, *IEEE Trans. Commun. Technol.* , pp. 162–165, Decr. 1964.
- [7] S. P. Lipshitz, R. A. Wannamaker, and J. Vanderkooy, Quantization and Dither: A Theoretical Survey, *J. Audio Eng. Soc.* , Vol. 40, No.5, pp. 355–375, May 1992.
- [8] R. A. Wannamaker, S. P. Lipshitz, J. Vanderkooy, and J. N. Wright, A Theory of Nonsubtractive Dither, *IEEE Trans. Signal Processing* , Vol. 48, No.2, pp. 499–516, Feb. 2000.
- [9] B. Widrow, Statistical Analysis of Amplitude-Quantized Sampled-Data Systems, *Trans. AIEE*, Pt. II: Appl. Ind., Vol. 79, pp.555 - 568, 1960.
- [10] A. B. Sripad, and D. L. Snyder, A Necessary and Sufficient Condition for Quantization Errors to be Uniform and White, *IEEE Trans. Acoust., Speech, Signal Processing*, Vol. ASSP-25, No. 5, pp. 442–448, Oct. 1977.
- [11] D.W. Chung and S.K. Sui, Analysis and Compensation of Current Measurement Error in Vector-Controlled AC Motor Drives, *IEEE Trans. Indust. Applicat.* , Vol. 34: No. 2, pp. 340–345, Mar./Apr. 1998.